

Modeling the Panchromatic Spectral Energy Distributions of Galaxies

Section 6,7,8

Charlie Conroy

December 18, 2019

Total Dust Attenuation

Four primary techniques:

- UV-to-NIR SED fitting (a known attenuation curve), constrain $E(B - V)_{\text{star}}$;
- Balmer decrement (an intrinsic ratio), e.g., $H\alpha/H\beta$, constrain $E(B - V)_{\text{gas}}$;
- Energy balance technique (statement), e.g., IRX- β relation;
- Using luminous background source with a known intrinsic spectrum, e.g., MW extinction (Fitzpatrick et al., 2019).

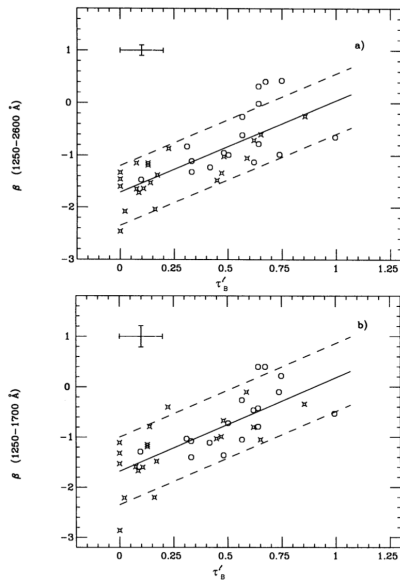
Commonly used parameterization: the total-to-selective attenuation curve

$$k_{\lambda} = \frac{A_{\lambda}}{E(B - V)},$$

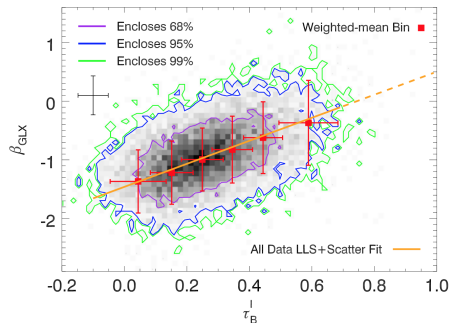
in which $E(B - V) = A_B - A_V$.

Nebular-to-stellar Attenuation Ratio

Calzetti et al. (1994)



Battisti et al. (2016)

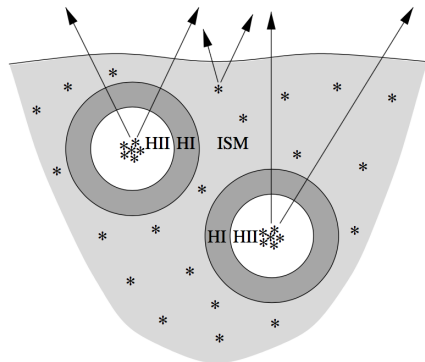


$$F(\lambda) \propto \lambda^\beta$$

$$\tau_B^l = \tau_{\text{H}\beta} - \tau_{\text{H}\alpha} = \ln \left(\frac{F(\text{H}\alpha)/F(\text{H}\beta)}{2.86} \right)$$

Calzetti (1997); Calzetti et al. (2000):
 $E(B-V)_{\text{star}} = (0.44 \pm 0.03) E(B-V)_{\text{gas}}$

Two-component Dust Model



Charlot & Fall (2000)

$$\tau_{\lambda}^{\text{tot}}(t) = \begin{cases} \tau_{\lambda}^{\text{BC}} + \tau_{\lambda}^{\text{ISM}} & t \leq t_{\text{BC}}, \\ \tau_{\lambda}^{\text{ISM}} & t > t_{\text{BC}}, \end{cases}$$

$$\tau_{\lambda}^{\text{BC/ISM}} = \tau_V^{\text{BC/ISM}} (\lambda/0.55\mu\text{m})^{-n}, \quad n = 0.7, \\ t_{\text{BC}} = 10 \text{ Myr}.$$

da Cunha et al. (2008): $n_{\text{BC}} = 1.3$,
 $n_{\text{ISM}} = 0.7$.

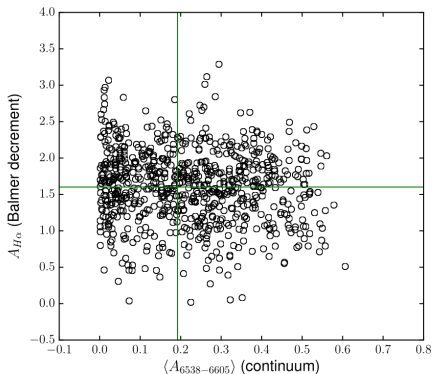
Whitmore et al. (2014): $t_{\text{BC}} \lesssim 10 \text{ Myr}$ in
 NGC 4038/39.

Hollyhead et al. (2015): $t_{\text{BC}} < 4 \text{ Myr}$ in
 M83.

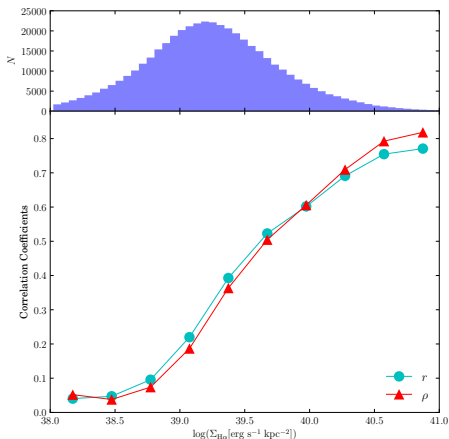
Grasha et al. (2019): $t_{\text{BC}} \lesssim 6 \text{ Myr}$ in M51.

$$\tau_{\lambda}^{\text{BC+ISM}} / \tau_{\lambda}^{\text{BC}} \text{ Ratio}$$

Viaene et al. (2017):
dust-lane ETGs

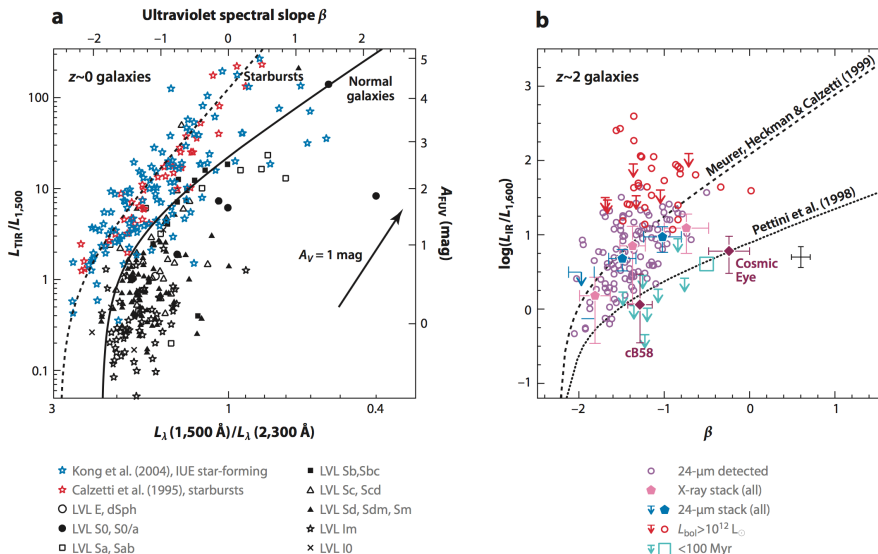


Lin & Kong (2019)



$\tau_{\lambda}^{\text{BC+ISM}} / \tau_{\lambda}^{\text{BC}}$ or $E(B - V)_{\text{star}} / E(B - V)_{\text{gas}}$ may be not a constant for all type of galaxies (Wild et al., 2011; Zahid et al., 2017; Koyama et al., 2019; Qin et al., 2019; Lin & Kong, 2019).

IRX- β Relation



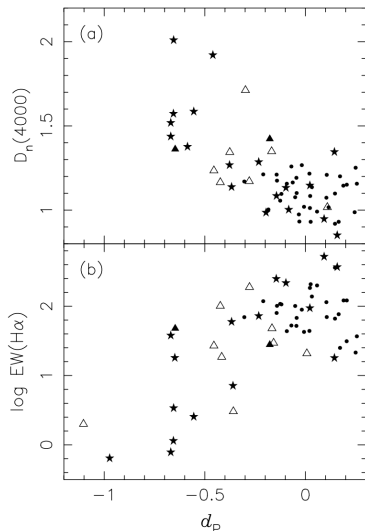
Second Parameter

- Kong et al. (2004): stellar population parameters (SFH)
- Boquien et al. (2009) (H II regions): dust geometries and extinction curves
- Casey et al. (2014): SFR (or L_{IR})

Disadvantage:

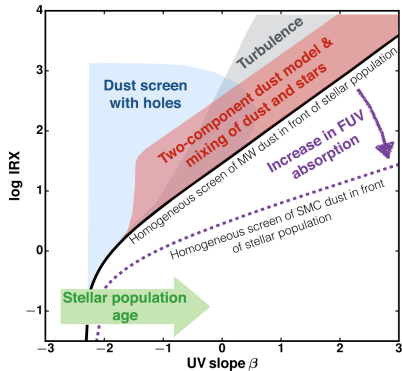
- Large uncertainties on IRX (Johnson et al., 2007)
- Energy balance statement might be broken at scale $\lesssim 1.5$ kpc (Williams et al., 2019)

Estimation of dust attenuation from the IRX- β will give way to more robust techniques.

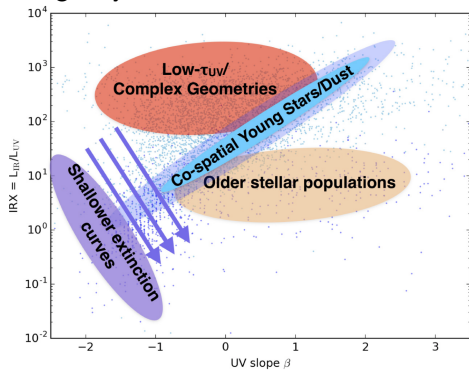


Origin of Scatter

Popping et al. (2017):
Starburst99+dust models



Narayanan et al. (2018): Cosmological
zoom galaxy formation simulations

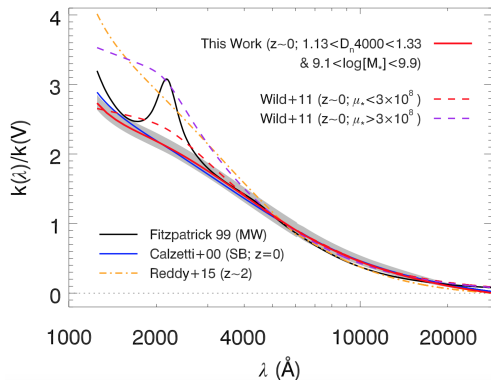


UV-to-NIR SED fitting

- Age–dust degeneracy: poorly constrained dust attenuation from UV-NIR broadband SEDs
- Break the degeneracy: spectroscopic or FIR data
- Narrow spectroscopic features: stellar age and metallicity, e.g., $D_n(4000)$ and $H\delta$ (Kauffmann et al., 2003)
- FIR data: measurement of the total L_{IR} (Noll et al., 2009a)

Constraints on the Attenuation Curve

- Calzetti et al. (1994, 2000): assuming the same underlying stellar populations, compare galaxies with different $\tau_B^l \rightarrow$ average attenuation curve for SB galaxies, shallower than the MW or LMC extinction curve, without 2175 Å bump
- Wild et al. (2011): pairs of galaxies with similar gas-phase metallicities, sSFRs, b/a but different τ_B^l
- Battisti et al. (2016); Battisti et al. (2017): local SFGs
- CIGALE fit for individual galaxies: Buat et al. (2018); Salim et al. (2018)
- High-z: Kriek & Conroy (2013); Reddy et al. (2015); Scoville et al. (2015); Zeimann et al. (2015); Cullen et al. (2018)



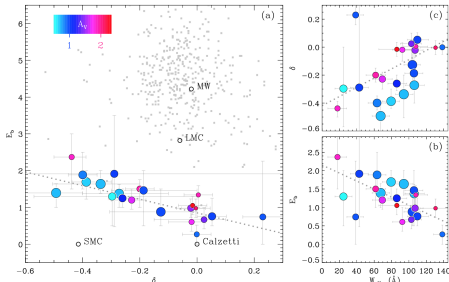
2175-Å dust feature

Expectation: normal SFGs should show evidence for the 2175 Å dust feature.
 Parameterize dust attenuation curve with a bump (Noll et al., 2009b):

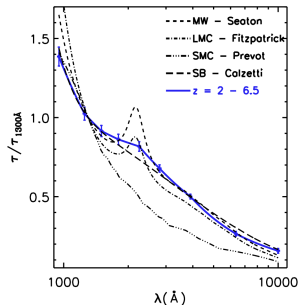
$$A(\lambda) = \frac{A_V}{4.05} (k_{\text{Cal}}(\lambda) + D(\lambda)) \left(\frac{\lambda}{\lambda_V} \right)^\delta$$

$$D(\lambda) = \frac{E_b(\lambda\Delta\lambda)^2}{(\lambda^2 - \lambda_0)^2 + (\lambda\Delta\lambda)^2}.$$

Kriek & Conroy (2013)

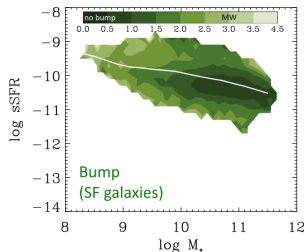
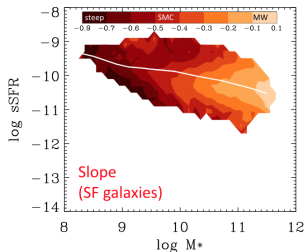
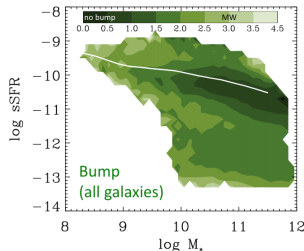
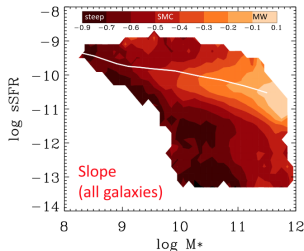


Scoville et al. (2015)



2175-Å dust feature

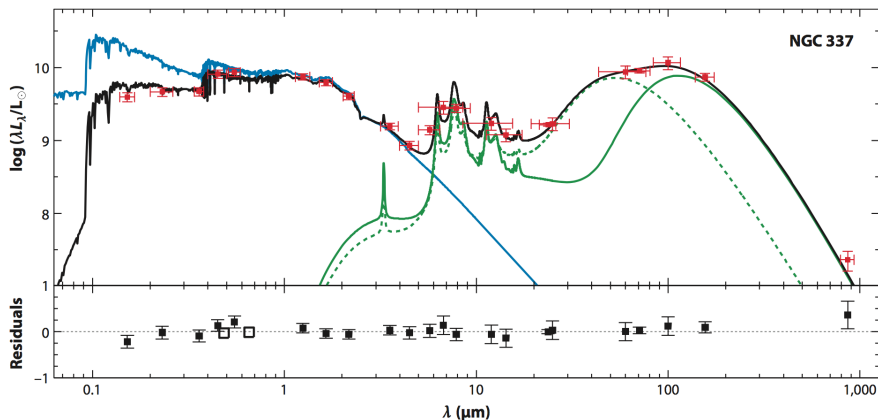
Salim et al. (2018): local galaxies, a wide range of UV bump amplitudes with an average strength of 1/3 of the MW bump.



Physical Dust Properties

Constraints on the M_{dust} and T_{dust} require data beyond the peak in the thermal dust emission spectrum at $\sim 100 \mu\text{m}$.

da Cunha et al. (2008) (MAGPHYS)



Physical Dust Properties

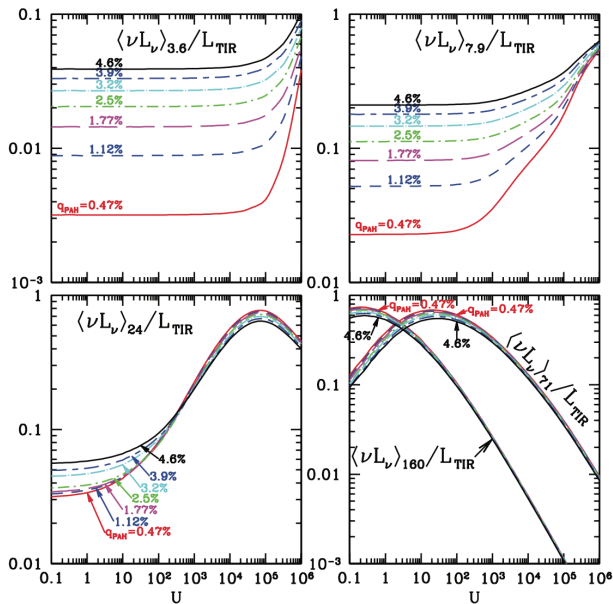
IR SED models:

Draine & Li (2007) (e.g., CIGALE)

- grain populations exposed to a variety of starlight intensities
- thermal emission and single photon heating of dust particles
- dust size distributions of MW (q_{PAH}) + emissivity for a dust mixture heated by $U + dM_{\text{dust}}/dU$
- free parameters: q_{PAH} , U_{min} , $\gamma(U > U_{\text{min}})$ (fixed $\alpha = 2$, $U_{\text{max}} = 10^6$, Draine et al. 2007)

With *Herschel* data: simplistic, modified blackbody dust models are no longer capable of providing adequate fits to the data.

Physical Dust Properties



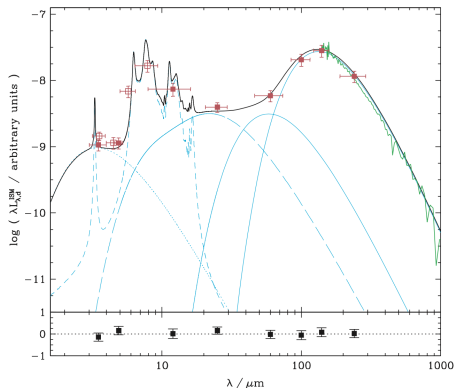
Physical Dust Properties

IR SED models:

da Cunha et al. (2008) (MAGPHYS)

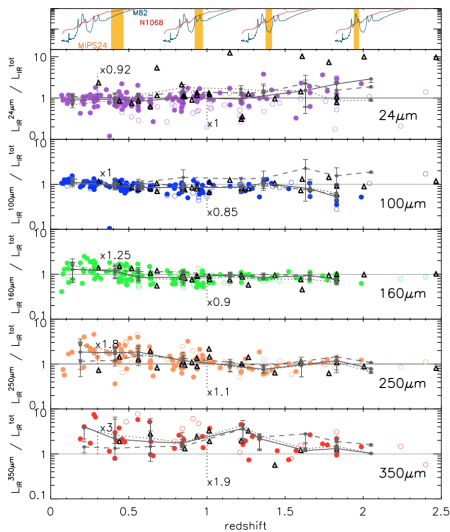
- an empirical spectrum for the PAH emission
- emission from stochastically heated grains
- warm and cold thermal dust

New update of MAGPHYS:
add 2175 Å bump to attenuation
curve (Battisti et al., 2019)

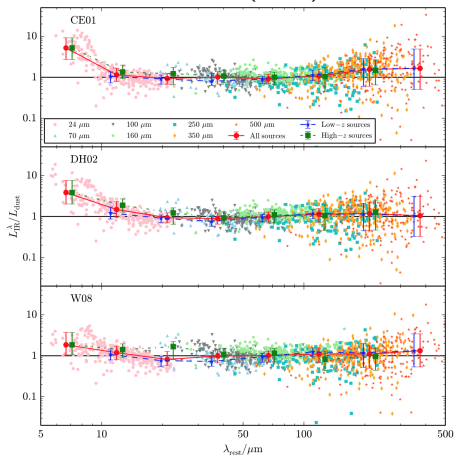


Cosmic Evolution of IR SEDs

MIR-excess problem (Elbaz et al., 2010)



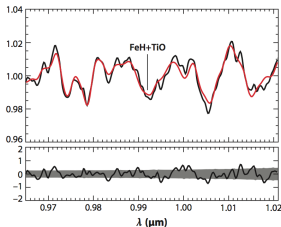
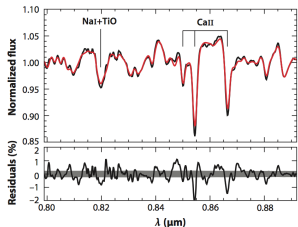
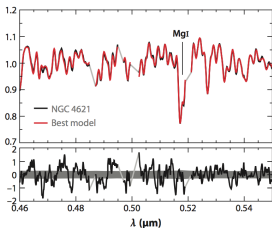
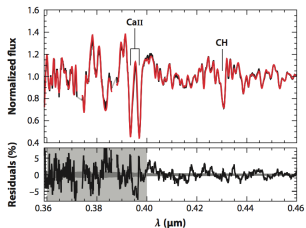
Lin et al. (2016)



Elbaz et al. (2011): local ULIRGs, a depressed emission component from PAHs due to hotter T_{dust} .

Constraints from SEDs

Problem: whether the IMF has had the same form over all of cosmic time and in all environments



- IMF-sensitive features: NaI doublet (0.82 μm), CaII triplet (0.86 μm), FeH band head (0.99 μm)
- Extremely dwarf-rich IMFs are now routinely ruled out.
- More modest IMF variations appear to be supported by the data, at the level of a factor of 2–3 in M/L.

Concluding Remarks

- Combining broadband data with moderate resolution spectra: IFU, narrow-band photometry, grism data (e.g., 3D-HST)
- Uncertainties in the SPS models are becoming a critical limiting factor to the interpretation of galaxy SEDs: include contributions from nebular emission and dust around AGB stars; FUV-FIR models, stellar evolution uncertainties
- A more sophisticated approach: derive the full posterior distributions via (e.g.,) MCMC techniques
- Understanding what is knowable from the modeling of galaxy SEDs

References I

- Battisti, A. J., Calzetti, D., & Chary, R.-R. 2016, *ApJ*, 818, 13
- Battisti, A. J., Calzetti, D., & Chary, R.-R. 2017, *ApJ*, 840, 109
- Battisti, A. J., da Cunha, E., Shivaeei, I., & Calzetti, D. 2019, 1912.05206v1
- Boquien, M., Calzetti, D., Kennicutt, R., et al. 2009, *ApJ*, 706, 553
- Buat, V., Boquien, M., Małek, K., et al. 2018, *A&A*, 619, A135
- Calzetti, D. 1997, in *American Institute of Physics Conference Series*, Vol. 408, American Institute of Physics Conference Series, ed. W. H. Waller, 403
- Calzetti, D., Armus, L., Bohlin, R. C., et al. 2000, *ApJ*, 533, 682
- Calzetti, D., Kinney, A. L., & Storchi-Bergmann, T. 1994, *ApJ*, 429, 582
- Casey, C. M., Scoville, N. Z., Sanders, D. B., et al. 2014, *ApJ*, 796, 95
- Charlot, S., & Fall, S. M. 2000, *ApJ*, 539, 718
- Cullen, F., McLure, R. J., Khochfar, S., et al. 2018, *MNRAS*, 476, 3218
- da Cunha, E., Charlot, S., & Elbaz, D. 2008, *MNRAS*, 388, 1595
- Draine, B. T., & Li, A. 2007, *ApJ*, 657, 810
- Draine, B. T., Dale, D. A., Bendo, G., et al. 2007, *ApJ*, 663, 866

References II

- Elbaz, D., Hwang, H. S., Magnelli, B., et al. 2010, *A&A*, 518, L29
- Elbaz, D., Dickinson, M., Hwang, H. S., et al. 2011, *A&A*, 533, A119
- Fitzpatrick, E. L., Massa, D., Gordon, K. D., Bohlin, R., & Clayton, G. C. 2019, *ApJ*, 886, 108
- Grasha, K., Calzetti, D., Adamo, A., et al. 2019, *Monthly Notices of the Royal Astronomical Society*, 483, 4707
- Hollyhead, K., Bastian, N., Adamo, A., et al. 2015, *Monthly Notices of the Royal Astronomical Society*, 449, 1106
- Johnson, B. D., Schiminovich, D., Seibert, M., et al. 2007, *ApJS*, 173, 392
- Kauffmann, G., Heckman, T. M., White, S. D. M., et al. 2003, *MNRAS*, 341, 33
- Kong, X., Charlot, S., Brinchmann, J., & Fall, S. M. 2004, *MNRAS*, 349, 769
- Koyama, Y., Shimakawa, R., Yamamura, I., Kodama, T., & Hayashi, M. 2019, *PASJ*, 71, 8
- Kriek, M., & Conroy, C. 2013, *ApJ*, 775, L16
- Lin, Z., Fang, G., & Kong, X. 2016, *AJ*, 152, 191

References III

- Lin, Z., & Kong, X. 2019, 1912.01851v1
- Narayanan, D., Davé, R., Johnson, B. D., et al. 2018, *MNRAS*, 474, 1718
- Noll, S., Burgarella, D., Giovannoli, E., et al. 2009a, *A&A*, 507, 1793
- Noll, S., Pierini, D., Cimatti, A., et al. 2009b, *A&A*, 499, 69
- Popping, G., Puglisi, A., & Norman, C. A. 2017, *MNRAS*, 472, 2315
- Qin, J., Zheng, X. Z., Wuyts, S., Pan, Z., & Ren, J. 2019, *MNRAS*, 485, 5733
- Reddy, N. A., Kriek, M., Shapley, A. E., et al. 2015, *ApJ*, 806, 259
- Salim, S., Boquien, M., & Lee, J. C. 2018, *ApJ*, 859, 11
- Scoville, N., Faisst, A., Capak, P., et al. 2015, *ApJ*, 800, 108
- Viaene, S., Sarzi, M., Baes, M., Fritz, J., & Puerari, I. 2017, *MNRAS*, 472, 1286
- Whitmore, B. C., Brogan, C., Chandar, R., et al. 2014, *The Astrophysical Journal*, 795, 156
- Wild, V., Charlot, S., Brinchmann, J., et al. 2011, *MNRAS*, 417, 1760
- Williams, T. G., Baes, M., De Looze, I., et al. 2019, *MNRAS*, 487, 2753
- Zahid, H. J., Kudritzki, R.-P., Conroy, C., Andrews, B., & Ho, I.-T. 2017, *ApJ*, 847, 18
- Zeimann, G. R., Ciardullo, R., Gronwall, C., et al. 2015, *ApJ*, 814, 162